Viser Technology Pte. Ltd.
Mechanical Engineering Science
DOI: 10.33142/mes.v3i1.4332

Research Article Open Access

Theoretical and Experimental Study on The Speed-up of Freight Train with Mixed Marshaling of Light and Heavy Vehicle

Xing ZHANG, Li LI*, Dabin CUI*, Yaodong FU, Haiyang GUO

School of Mechanical Engineering, Southwest Jiaotong University, Chengdu, China

***Corresponding Author:** Li LI, Dabin CUI; No.111, North 1st Section, 2nd Ring Road, Chengdu City, 610031, China; lily1cn@aliyun.com, cdb1645@163.com*

Abstract:
To study the influence of the speed-up of a freight train with mixed marshaling of light and heavy vehicles on the dynamic behavior, a dynamic model of the freight train was established based on the modular method of cyclic variables, and the dynamic behavior of the freight train was simulated and analyzed under different marshaling patterns, speeds and line conditions. On-site speed-up test with different marshaling freight trains was carried out, and the stability and ride-index of the train before and after the speed-up were compared and analyzed. The feasibility of increasing the speed of freight trains with mixed marshaling of light and heavy cars was demonstrated theoretically and experimentally. The results show that the theory is in good agreement with the test, which can effectively reflect the dynamic behavior of the vehicle. The dynamic behavior of the freight train in the study meets the requirements of increasing speed to 90 km/h. This paper provides a theoretical basis and method for railway freight transportation and the speed-up of freight vehicles.

Keywords: *Mixed marshaling of light and heavy vehicle; Freight train; Dynamic behavior*

1 Introduction

As a large logistics transportation, freight train has an important impact on my country's development [1-2]. The speed of freight trains is the key factor that restricts transportation efficiency. With the increase of speed, it will greatly affect the smoothness and stability of the train operation. Some scholars have done a study on the effect of the speed-up of a freight train on the structure and dynamic performance. Liu [3] analyzed the structure, performance, and problems existing in the application of the current Z8AG, Z8G, ZK2, and swing bogies. Wu et al.[4] established the dynamic model of the nonlinear system and the finite element model of the side frame, and studied its fatigue life. Based on the Bayesian method and the reliability analysis method, Chen et al.[5] used the reliability analysis method to systematically study the lateral dynamic performance of the speed-up of a freight train on circular lines. Gong et al.[6] proposed an evaluation method for strengthening railway track structure based on the anti-derailment safety degree of a freight train. Chen et al.[7] carried out the 120 km/h comprehensive speed increase test of a freight train, and compared the test lines, vehicles, operating characteristics. Zhan et al.[8] made statistics and analysis of the problems found in various parts of a freight train in the maintenance process, and summed up the influence of the speed-up of a freight train. Qin [9] elaborated on the influence of the speed-up on a freight train and put forward targeted maintenance suggestions. To improve the safety of the vehicle operation, Xue [10] studied the lateral motion stability of the speed-raising locomotive and vehicle. Li et al.[11] improved the wheel-rail relationship of speed-increasing on the vehicle, and studied the MBS co-simulation of the dynamic design of bogies. Fu et al.[12] studied the dynamic behavior of key parameters of the steering frame on the vehicle, and gave the design scheme of speed-increasing. Under the background of speeding up and freight transport in China, Wu [13] pointed out the transformation and development direction of the speed-up of a freight train.

The above results have laid an important foundation for studying the influence of the speed-up on the dynamic performance of freight trains with mixed marshaling of light and heavy cars. However, most of the previous studies focused on the vehicle system and tended to focus on the influence of the speed-up on vehicle structure. Few studies have been conducted on the combination of theoretical calculation and experimental verification of the speed-up of empty-heavy mixed freight trains.

Received 25 February 2021; Accepted 28 April 2021

To improve the transportation capacity, this paper takes section lines and mixed freight trains with mixed marshaling of light and heavy cars as the object, and establishes the dynamic model of the long and large marshaling train based on the modular method of cyclic variables. The simulation analysis of the dynamic performance of the freight train is carried out. Under the guidance of a theoretical study, the test on the speed-up of the freight train in this section is completed.

2 Theoretical study

2.1 The modeling of vehicle dynamics

A freight train consists of at least dozens of vehicles. If a train contains n vehicles, and each vehicle has m degrees of freedom, then the whole system has $m \times n$ degrees of freedom. The equation of the system is expressed as follows:

$$[M]\ddot{Y} + [C]\dot{Y} + [K]Y = \{P\} + \{F\} \quad (1)$$

Among them, $[M]$is the mass matrix of the system, $[C]$ is the damping matrix of the system, $[K]$ is the stiffness matrix of the system, Y is the degree of freedom variable of the train, $\{P\}$ is the external force of the train, $\{F\}$ is the interaction force between vehicles.

Due to the long marshaling of freight trains, the traditional multi-rigid body dynamics modeling method will lead to " freedom explosion " and bring great difficulties to the calculation and analysis. Therefore, a modular method based on cyclic variables is developed to model and solve the dynamics of the long marshaling train [14]. Equation (1) could be decomposed into n sub-equations:

$$[m_i]\{\ddot{Y}_i\} + [c_i]\{\dot{Y}_i\} + [k_i]\{Y_i\} = \{p_i\} + \{f_i\} \quad (2)$$

Where, $\{Y_i\}$ is the set of the degree of freedom of the i^{th} vehicle, $[m_i]$ is the mass matrix of the i^{th} vehicle, $[c_i]$ is the damping matrix of the i^{th} vehicle, $[k_i]$ is the stiffness matrix of the i^{th} vehicle, $[p_i]$ is the external force acting on the i^{th} vehicle, and $[f_i]$ is the interaction force between the vehicles.

According to equation (2), a train can be regarded as an integral unit, and the system is divided into n basic integral units for calculation separately, and the calculation of each vehicle uses the same set of the degree of freedom variables. After the calculation of each vehicle is completed, the result is stored in the transfer variable, then the degree of freedom variable is released for the calculation of the next vehicle until all vehicles have completed the calculation. The next integration step is still carried out in the mode of the previous integration step until all the integration calculations are completed. In the integral calculation of the whole train, the degree of freedom variable will not increase with the increase of train formation, so it can solve the problem caused by the "degree of freedom explosion" of the long marshaling train. This method is called the "cyclic variable method".

The cyclic variable method is only good at solving the modeling of long marshaling train with only one type, but it is difficult to solve mixed train with many types. In the actual operating train, especially freight train, mixed marshaling often occurs. For this purpose, a locomotive and rolling stock model library (which can include all types of rolling stock) is established, and the dynamic simulation of the whole train can be performed by setting the sequence number of the corresponding vehicle type according to the train composition. When the train formation changes, there is no need to remodel and modify the program, just modify the definition of the formation, which greatly facilitates the modeling of the mixed train. This method is called "modular modeling".

Based on the modular modeling method of cyclic variables, the TPL train multi-body dynamics software is used for modeling, in which K2 bogie is selected for the empty train bogie, and the dynamics of a mixed freight train with light and heavy cars are simulated.

2.2 The analysis of dynamic performance

Using the American pentad spectrum for excitation, the dynamics of different trains when passing through the straight line and curve at the speed of 80 km/h, 85 km/h, and 90 km/h, as well as the dynamics of common braking and the emergency braking, are simulated. The stability of the train in the process of the speed-up is analyzed comprehensively, and the maximum value of the evaluation indexes of each group is calculated under different operating conditions and line conditions. The marshaling situation is as follows:

Croup 2: locomotive +16 heavy vehicles +5 empty vehicles +23 heavy vehicles +5 empty vehicles +16 heavy vehicles;

Group 3: locomotive +5 empty vehicles +55 heavy vehicles +5 empty vehicles;

Group 4: locomotive +55 heavy vehicles +10 empty vehicles;

Group 5: locomotive +27 heavy vehicles +10 empty vehicles +28 heavy vehicles.

The whole train is numbered with the locomotive as the starting position, that is, the locomotive number is 0, and the tail train number is 65.

The straight line is used to calculate the stability. Each group passes at the speed of 80 km/h, 85 km/h, and 90 km/h respectively in three passing modes (traction condition, common braking, and emergency braking) to obtain lateral and vertical stability. By comparing the stability at a different speed, it is found that the lateral stability and the vertical stability both increase with the increase of speed. Therefore, the maximum value of the lateral stability and the vertical stability of each marshaling is taken, as shown in Fig.1 and Fig.2 respectively. The red line with the value of 3.5 indicates that the index of a freight train is "excellent".

As can be seen from Fig.1, in the traction condition, for empty vehicles in the middle position, the lateral stability of group 2 decreases in the part of empty vehicle number (17-21, 45-49), while that of group 5 decreases in the first half of empty vehicle number (28-32), and increases in the latter part of empty vehicle number (33-38). However, for the empty vehicles at both ends of the position, the lateral stability of group 3 and group 4 increases when the

empty vehicles are numbered respectively. In the traction condition, empty vehicles should be placed in the middle position as far as possible, and the number of continuous empty vehicles should not be too many, which can effectively reduce the lateral stability. In common braking and emergency braking, the lateral stability of each group increases in the number of their respective empty vehicles. In common braking, because the speed reduces slowly, the vibration of the empty part is more balanced, so the lateral stability of the empty part of each group is not much different; However, in emergency braking, the pressure of the empty part becomes larger due to the extrusion of the front vehicle by the rear vehicle, resulting in the lateral stability of the empty vehicle with the rear number being greater than that of the empty vehicle with the front number. The maximum lateral stability of each group does not exceed the prescribed limit, reaching the "excellent".

As can be seen from Fig.2, for group 3 and group 4 with empty vehicle numbers at the rear, the vertical vibration becomes larger due to the lightweight of empty vehicles at the end. Under traction conditions, common braking, and emergency braking, the vertical stability of group 3 and group 4 decreases successively, and the vehicle number when the vertical stability begins to increase gradually falls back. When the two ends of empty vehicles are connected with heavy vehicles, the vertical vibration of empty vehicles will be suppressed, so the vertical stability of group 2 and group 5 is small. The maximum vertical stability of each group does not exceed the prescribed limit, reaching the "excellent".

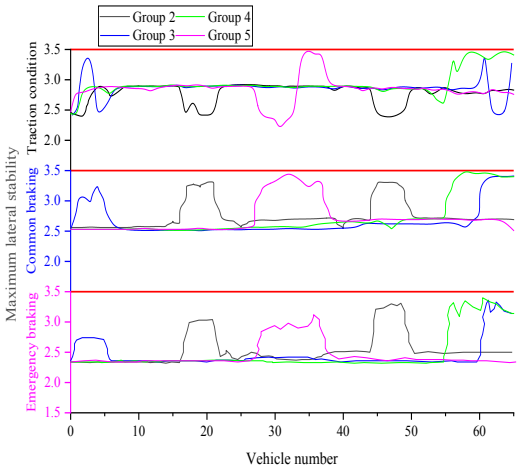

Fig.1 Maximum lateral stability

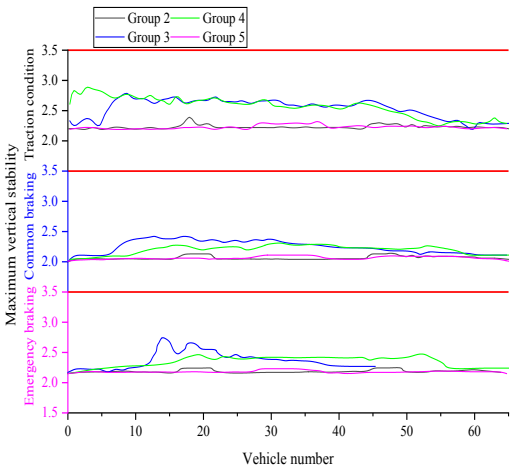

Fig.2 Maximum vertical stability

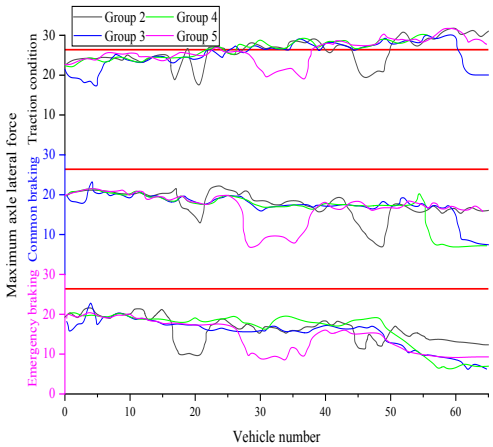

Fig.3 Maximum axle lateral force

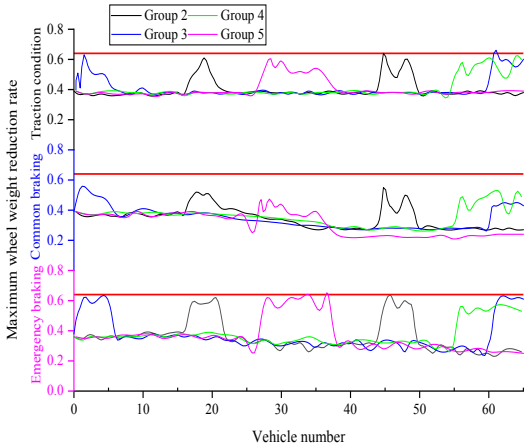

Fig.4 Maximum wheel weight reduction rate

When the axle lateral force is calculated, it is divided into a straight line and curve. The radius of the curve is R=600 m, and the length of the transition curve is 110 m. In common braking, the decompression is 70 kPa. Each group passes through the straight line and curve at the speed of 80 km/h, 85 km/h, and 90 km/h under three passing modes (traction condition, common braking, and emergency braking), and the lateral force of the three passing modes are obtained respectively. After the statistics are done, it is found that at the same speed, the higher the speed is when crossing the curve, the more obvious it is squeezed by the outer rail. Therefore, under the three passing modes, the lateral force reaches its maximum value at the curve and the speed of 90 km/h. Therefore, this state represents the

maximum lateral force, as shown in Fig.3. The red line with the value of 26.4 represents the upper limit of the calculated lateral force as “excellent”.

As can be seen from Fig.3, in the three passing modes, the axle lateral force of each group decreases in the number part of the empty vehicle. When passing through the curve without braking, the extrusion of the outer rail is the most obvious because of the high speed. As for the common braking and emergency braking, the lateral force of the rear wheel is significantly reduced due to the gradual decrease of the speed when passing through the curve. In the case of traction condition, the maximum axle lateral force of each group is close to the value of 26.4, and the other cases do not exceed the upper value of 26.4, reaching the “excellent”.

When calculating the wheel weight reduction rate, it is divided into straight lines and curves, the radius of the curve is R=600 m, and the length of the transition curve is 110 m. In common braking, the decompression is 70 kPa. Each group passes through the straight line and curve at the speed of 80 km/h, 85 km/h, and 90 km/h under the three passing modes (traction condition, common braking, and emergency braking), and the wheel reduction rate of the three passing modes are obtained respectively. After the statistics, it is found that at the same speed, the wheel weight reduction rate is larger when crossing the curve. The higher the speed is, the greater the wheel weight reduction rate is. Under the three passing modes, the wheel weight reduction rate reached its maximum value at the curve and the speed of 90 km/h, so this state is taken to represent the maximum wheel weight reduction rate, as shown in Fig.4. The red line with a value of 0.64 in the Fig. indicates that the wheel weight reduction rate is the "first limit".

As can be seen from Fig.4, in the three passing modes, due to the lightweight of the empty vehicle, the wheel weight reduction rate of each group increases in its empty vehicle number part. Under the traction condition, because the speed remains unchanged, the wheel weight reduction rate of each group remains unchanged. Under common braking and emergency braking, the wheel weight reduction rate of each group decreases gradually due to the decrease of speed. The maximum wheel weight reduction rate of each group in the empty vehicle number part is close to 0.64, and the other cases do not exceed the upper limit, reaching the “first limit”.

When calculating the derailment coefficient, it is divided into the straight line and curve, the radius of the curve is R=600 m, and the length of the transition curve is 110 m. In common braking, the decompression is 70 kPa. Each group passes through the straight line and curve at the speed of 80 km/h, 85 km/h, and 90 km/h under three passing modes (traction condition, common braking, and emergency braking), and the derailment coefficient of the three passing modes are obtained respectively. The derailment coefficient when passing through the curve at the speed of 90 km/h is the maximum under the three passing modes, as shown in Fig.5. The red line with the value of 1.2 indicates that the calculated derailment coefficient is the “first limit”.

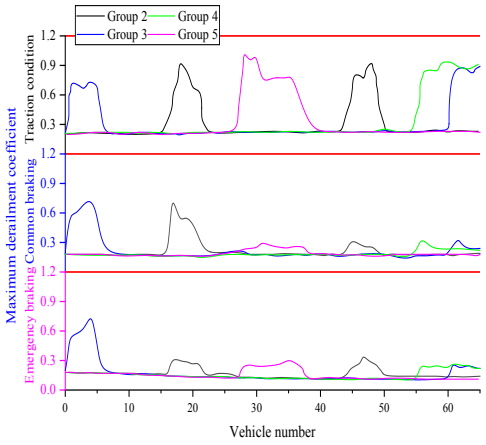

Fig.5 Maximum derailment coefficient

As can be seen from Fig.5, under the traction condition, the derailment coefficients of all groups in the empty part increase as the train pass through the curve at the speed of 90 km/h. For common braking and emergency braking, the speed begins to decrease when crossing the curve, so the part at the back of the empty train number decreases rapidly, finally is close to the derailment coefficient of the heavy train part. The maximum derailment coefficient of each group does not exceed the upper limit, reaching the “first limit”.

3 Experimental study

3.1 Experimental method

Vehicle dynamics test refers to the calculation of derailment coefficient and other dynamic performance based on the measured data of <GB/T 5599-1985 Code for Dynamic Performance Evaluation and Test Identification of Railway Vehicles> using a force measuring wheelset. Fig.6 shows the force measuring wheelset and data acquisition equipment in the test site.

(a) Force measuring wheelset

(b) Data acquisition equipment

Fig.6 Vehicle dynamics test site drawing

The wheel-rail lateral force Q and wheel-rail vertical force P are measured by force measuring wheels [15-16]. 4 force measuring wheelsets are selected, and the tread wear state is 2 new spins, and the other 2 wheels is abrasion value of 3mm. The measuring patch layout is shown in Fig.7.

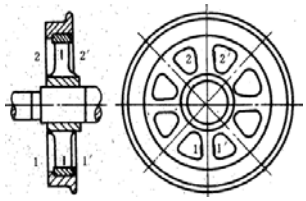

(a) Vertical force measurement

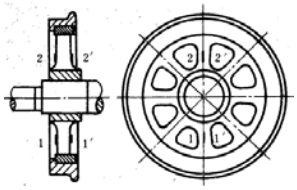

(b) Lateral force measurement

Fig.7 The measuring patch position

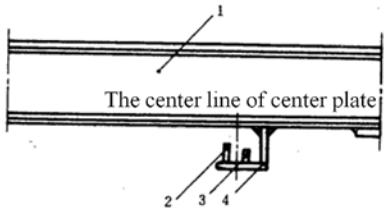

Fig.8 Acceleration sensor installation diagram

Fig.8 shows the installation diagram of the acceleration sensor. The acceleration sensor for measuring the vertical and lateral acceleration of the train body is installed on the lower cover plate of the middle beam of the chassis of the 1 or 2 inner core plate which is less than 1000 mm from the centerline of the core plate. Among them, 1 is the middle beam, 2 and 3 are the vertical and lateral acceleration sensors, and 4 is the installation iron.

After getting data, the proportional coefficient $K_p$and K_q of vertical and lateral force and their mutual influencing factors E_{qp} and E_{pq} can be obtained from Equation 3-6.

Vertical force proportional coefficient:

$$K_p = \varepsilon_{pp}/P \tag{3}$$

Lateral force proportional coefficient:

$$K_q = \varepsilon_{qq}/Q \tag{4}$$

The influence coefficient of vertical force on lateral force bridge:

$$E_{qp} = \varepsilon_{qp}/P \tag{5}$$

The influence coefficient of lateral force on vertical force bridge:

$$E_{pq} = \varepsilon_{pq}/Q \tag{6}$$

You can get the coefficient matrix $K = \begin{vmatrix} K_p & E_{qp} \\ E_{pq} & K_q \end{vmatrix}$, and calculate its inverse matrix K^{-1}, and take the first group of the strain of the right wheel as an example, the calculation formula of vertical force P and lateral force Q is as follows:

$$P = K^{-1}(1,1) \times A(:,1) + K^{-1}(1,2) \times A(:,2) \tag{7}$$

$$Q = K^{-1}(2,1) \times A(:,1) + K^{-1}(2,2) \times A(:,2) \tag{8}$$

In the equation, *A(:,1)* is the first group of the vertical strain of the right wheel, and *A(:,2)* is the first group of the lateral strain of the right wheel.

3.2 The analysis of data

To select the most dangerous test section for the subsequent reciprocating test, the vertical force and lateral force of the wheels are collected through the whole line pull test with no load. Vehicle dynamics tests are carried out on group 2, group 3, group 4, and group 5, and the measured results are averaged, and the maximum value of the data in this group is taken as the upper limit of the error bar. The result is shown in Fig.s 10-15. In Fig. 2, Fig. 3, Fig. 4, and Fig. 5 represent group 2, group 3, group 4, and group 5 respectively; NB, CN, and EB respectively represent traction condition, common braking, and emergency braking; CT4 and CT5 represent the whole-course pull test of group 4 and group 5, respectively.

Fig.9 and Fig.10 respectively show the axle lateral forces of group 2, group 3, group 4, and group 5 when passing through straight lines and curves. The red line of 26.4 represents the upper limit of the calculated axle lateral force. Under the same condition, the axle lateral force at the curve is larger, the reason is that the lateral component force generated by centrifugal force is larger. When passing through the straight line, the axle lateral force of group 3 and group 4 is relatively small under the traction condition, the reason is that there is no extrusion of the front and rear vehicles, and the vehicles run smoothly. Under common braking, the rear train will squeeze the front train, causing the axle lateral force larger; In emergency braking, its characteristics are similar to those of common braking in the absence of relatively insufficient rear braking. However, in the case of relatively insufficient rear braking, the rear wheels of the test vehicle will be squeezed and the axle lateral force will increase. When passing through the curve, the axle lateral force is small under the common braking, and the reason is that the speed decreases and the wheel subjected to the rail force decreases. Due to the whole pull-on test of group 4 and group 5, their lines contain straight lines and curves, and their maximum value appears in the curve section, so their derailment coefficient is larger. There is no obvious rule for each test parameter of the vehicles running at different speed levels, which might be similar running speed levels, and there is a certain speed error in the actual running, that is, 80 km/h is between 79-82 km/h, 85 km/h is between 83-87 km/h, and 90 km/h is between 88-90 km/h. The maximum axle lateral force of each group does not exceed 26.4, reaching the "excellent".

Fig.11 and Fig.12 respectively show the wheel weight reduction rate of group 2, group 3, group 4, and group 5 when passing through the straight line and curve. The red line with the value of 0.64 represents the "first limit" of the wheel weight reduction rate. In the same case, due to the greater effect of the outer rail on the wheel when

passing through the curve, the vertical component force between the wheel and the rail increases, then the wheel weight changes greatly. When passing through the straight line, the wheel weight reduction rate is small under the traction condition, because the extrusion pressure of each group is small before and after the vehicle in the absence of braking. In common braking and emergency braking, the rear vehicle squeezes the front vehicle, resulting in a larger wheel weight reduction rate. With the increase of the speed of each vehicle, the wheel weight reduction rate becomes larger. When passing the curve, the higher the speed is, the higher the wheel weight reduction rate is. At the same speed, the wheel weight reduction rate in the traction condition is higher than that in the braking condition. This is because the wheelset load reduction caused by the vehicle passing at a higher speed is greater than that caused by the extrusion of the front and rear vehicles due to braking. Since group 4 and group 5 are carried out the whole pull-on test, their lines contain a straight line and curve, and its maximum value appears in the curve section, so the maximum value is obtained when passing through the straight line and the curve. The wheel weight reduction rate of each group is no more than 0.64, reaching the "first limit".

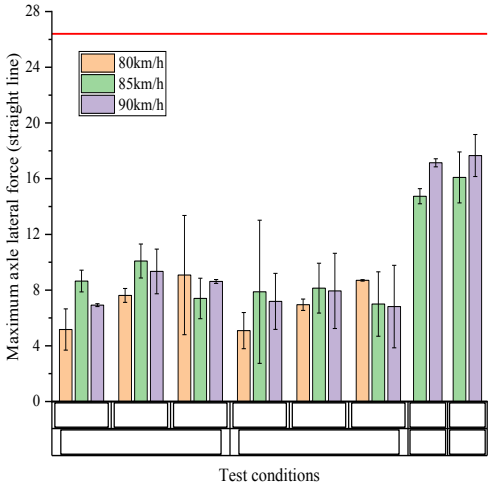

Fig.9 Maximum axle lateral force (straight line)

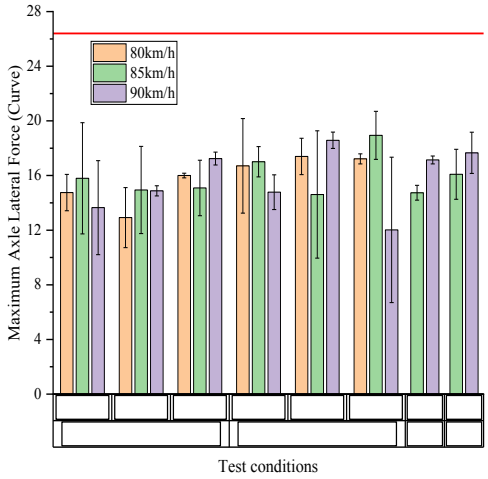

Fig.10 Maximum axle lateral force (curve)

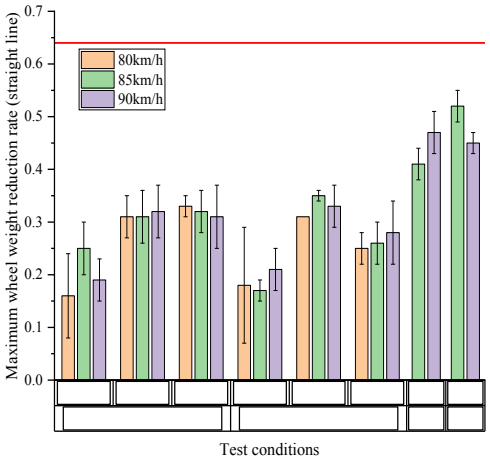

Fig.11 Maximum wheel weight reduction rate (straight line)

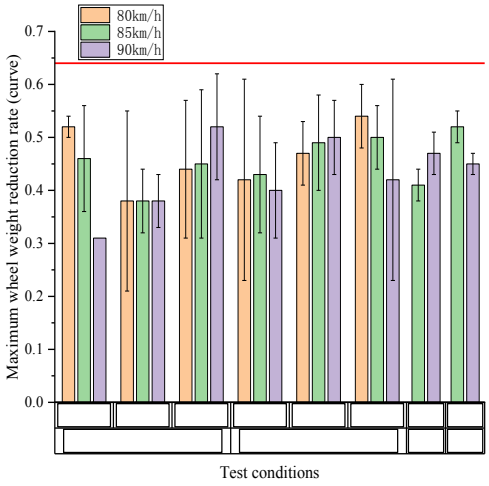

Fig.12 Maximum wheel weight reduction rate (curve)

Fig.13 and Fig.14 respectively show the derailment coefficient of group 2, group 3, group 4, and group 5. The red line with the value of 1.2 indicates that the derailment coefficient is the "first limit". In the same case, the derailment coefficient is larger when passing through the curve than when passing through the straight line. When passing through the straight line, under the same marshaling mode, there is no obvious rule of test parameters for each marshaling vehicle running at different speed levels. When passing through the curve, compared with the traction condition, the speed of common braking decreases gradually, so the derailment coefficient is low. Compared with emergency braking, the extrusion pressure of front and rear vehicles under common braking is smaller, so the derailment coefficient is smaller. Group 4 and group 5 are carried out the whole pull-on test. The circuit of

group 5 included the straight line and the curve, and its maximum value appeared in the curve section. Therefore, the maximum value is obtained when passing through the straight line and the curve, so the value in Fig.13 and Fig.14 is the same. The derailment coefficient of each group does not exceed the upper limit, reaching the "first limit".

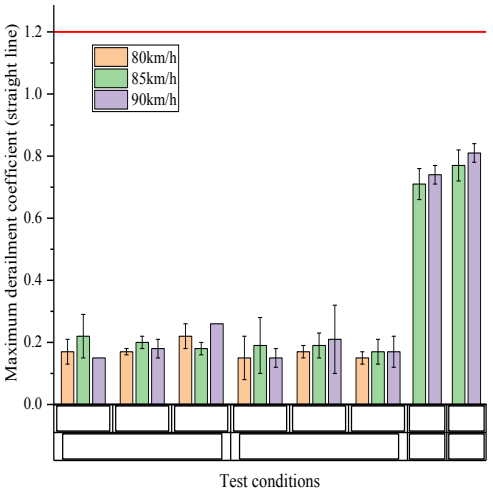

Fig.13 Maximum derailment coefficient (straight line)

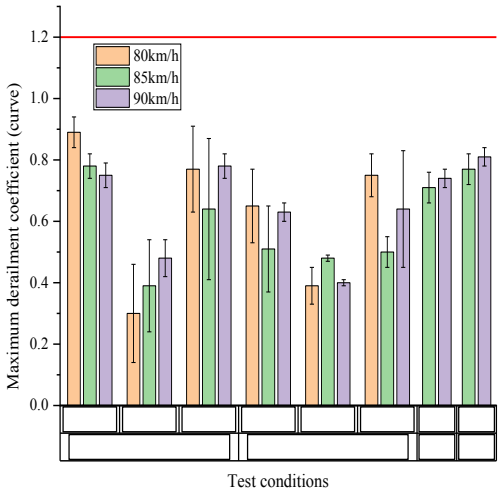

Fig.14 Maximum derailment coefficient (curve)

4 Conclusion

Based on the modular modeling method, the dynamic model of the long marshaling empty-heavy mixed freight train is established, and the dynamic characteristics of the vehicle system under different marshaling modes and operating conditions are discussed theoretically. The result shows that the dynamic performance of empty freight trains is lower than that of heavy freight trains due to the longitudinal impulse action during the traction and braking process, and the dynamic performance of empty freight trains is the worst when it is in the rear position. Based on the theoretical calculation, the experimental tests are carried out under conditions with bad dynamic performance. The result shows that the theoretical calculation is in good agreement with the experimental tests. In the selected speed-up section, all the dynamic performance indexes of the empty-heavy mixed freight train meet the speed-up requirements. Therefore, theoretical calculation and experimental test can complement and verify each other, and provide an important guarantee for reasonable speed-up of freight train.

Acknowledgments: The authors gratefully acknowledge the support of the School-enterprise cooperation projects (No.20200203)

References

[1] Zhai W, Cai C, Wang Q, Lu Z, Wu X. Dynamic effects of speed-raise train on the track and the countermeasures 2000(03): 13-22.

[2] Yu S. Analysis on the influence of railway freight train speed increase on vehicles and study on maintenance opinions 2019(05): 154-155.

[3] Liu Z. Bogie structures of speed-rising freight train 2003(03): 286-289.

[4] Wu P, Wen S, Wang J, Lan Q. Fatigue life prediction on the side frame of ZK2 bogie of the speed-increased freight train 2009, 30(01): 91-95.

[5] Chen L, Lu K, Yu W, Wang H. Reliability analysis method for the lateral dynamics performance of the speed-increased wagon 2009, 30(03): 97-102.

[6] Gong K, Xiang J, Liu L. Track strengthening measures assessment of heavy haul railway based on freight train anti-derailment safety degree 2020, 51(03): 832-841.

[7] Chen L, Wang X. Analysis of the dynamic performance of the 120 km/h speed increased comprehensive testing freight trains 2007(08): 27-34+55-56.

[8] Zhan H. Influence analysis and maintenance suggestions of railway freight train speed increase on vehicles 2015, 13(10): 56.

[9] Qin Z. Influence of speed boost of the railway on freight trains 2014(04): 208-209.

[10] Xue P. Research and application of lateral movement stability of accelerated locomotive and vehicle 2019, 5(09): 193-194.

[11] Li T, Wang Q, Piao M. Wheelset self-stability and MBS simulations of speeding-up railway 2021, 38(02): 103-109.

[12] Fu B, Luo S, Ma W, Tang Y. Dynamic analysis of key parameters of bogie to speed-raising metro vehicle 2018(01): 12-14+18.

[13] Wu Y. Improvement and development direction of railway freight train speedup in china under the background of speedup 2008, 24(3): 70-71.

[14] Chi M, Jiang Y, Zhang W, Wang Y. System dynamics of long and heavy haul train 2011, 11(03): 34-40.

[15] Yang X, Chen J. Wheel rail force measurement method based on wheel and axle strain 2014(08): 141-142.

[16] Ren Y, Chen J, Lin J. A blind signal separation based measurement of the wheel/rail force of an instrumented wheelset 2010, 29(3): 289-292.